Use of single-component wind speed in Rankine-Hugoniot analysis of interplanetary shocks

Vasiliy S. Vorotnikov,[1] Charles W. Smith,[2] Charles J. Farrugia,[2] Calum J. Meredith,[3] Qiang Hu,[4] Adam Szabo,[5] Ruth M. Skoug,[6] Christina M. S. Cohen,[7] Andrew J. Davis,[7] and Kiyohumi Yumoto[8]

Received 28 September 2010; revised 31 January 2011; accepted 3 February 2011; published 1 April 2011.

[1] We have extended and deployed a routine designed to run independently on the Web providing real-time analysis of interplanetary shock observations from L_1. The program accesses real-time magnetic field, solar wind speed, and proton density data from the Advanced Composition Explorer (ACE) spacecraft, searches for interplanetary shocks, analyzes shocks according to the Rankine-Hugoniot (R-H) jump conditions, and provides shock solutions on the Web for space weather applications. Because the ACE real-time data stream contains the wind speed but not the three-component wind velocity, we describe modifications to the R-H analysis that use the scalar wind speed and show successful results for analyses of strong interplanetary shocks at 1 AU. We compare the three-component and one-component solutions and find the greatest disagreement between the two rests in estimations of the shock speed rather than the shock propagation direction. Uncertainties in magnetic quantities such as magnetic compression and shock normal angle relative to the upstream magnetic field show large uncertainties in both analyses when performed using an automated routine whereas analyses of the shock normal alone do not. The automated data point selection scheme, together with the natural variability of the magnetic field, is inferred to be a problem in a few instances for this and other reasons. For a broad range of interplanetary shocks that arrive 30 to 60 min after passing L_1, this method will provide 15 to 45 min of advanced warning prior to the shock's collision with the Earth's magnetopause. The shock, in turn, provides advance warning of the approaching driver gas.

Citation: Vorotnikov, V. S., C. W. Smith, C. J. Farrugia, C. J. Meredith, Q. Hu, A. Szabo, R. M. Skoug, C. M. S. Cohen, A. J. Davis, and K. Yumoto (2011), Use of single-component wind speed in Rankine-Hugoniot analysis of interplanetary shocks, *Space Weather*, *9*, S04001, doi:10.1029/2010SW000631.

1. Introduction

[2] In a previous article [*Vorotnikov et al.*, 2008] we describe a scheme for the automated analysis of interplanetary shocks that could be useful in space weather applications. The practical motivations for providing such information prior to the arrival of shocks at the Earth's magnetosphere are described there. If we include the shock as a precursor to the driver gas with properties that are at least in part determined by the speed, density, and magnetic field of the driver gas, then real-time analysis of the shock provides an early warning for transients that can perturb the magnetospheric field inducing voltage and current spikes along electrical wires and pipelines, enhance radiation belts, destroy unprotected electronics, create negative environments for astronauts, and provide other space weather responses that adversely effect a modern technological society. Several articles published

[1]Department of Chemical Engineering, University of New Hampshire, Durham, New Hampshire, USA.
[2]Space Science Center, Institute for the Study of Earth, Oceans, and Space, Physics Department, University of New Hampshire, Durham, New Hampshire, USA.
[3]Department of Physics and Astronomy, University of Leicester, Leicester, UK.
[4]CSPAR, University of Alabama in Huntsville, Huntsville, Alabama, USA.
[5]Code 672, NASA Goddard Space Flight Center, Greenbelt, Maryland, USA.
[6]Los Alamos National Laboratory, Los Alamos, New Mexico, USA.
[7]Space Radiation Laboratory, California Institute of Technology, Pasadena, California, USA.
[8]Space Environment Research Center, Kyushu University, Fukuoka, Japan.

more recently suggest interesting additional applications and symbioses [*Balch*, 2008; *Sun et al.*, 2008; *Smith et al.*, 2008; *Yu and Ridley*, 2008; *Huttunen et al.*, 2008]. The Huttunen et al. analysis is especially interesting as it argues that the sheath region behind the shock is most effective in driving geomagnetically induced currents. The computed shock parameters (density compression and shock normal) together with upstream solar wind parameters are indicators of the turbulence level within the downstream sheath region and so analysis of the shock parameters in real time can provide advance warning of the intensity of the approaching sheath.

[3] We have now implemented the automated shock detection and analysis software using real-time data from the Advanced Composition Explorer (ACE) as provided by the NOAA/SWPC facility (at http://www.swpc.noaa.gov/ace/). One critical limitation in the ACE real-time data stream escaped our notice when preparing *Vorotnikov et al.* [2008] that could have proven highly detrimental to the effort of providing real-time shock analyses: the ACE real-time solar wind data contains the wind speed, but not the full three-component velocity [*Zwickl et al.*, 1998]. The Rankine-Hugoniot (R-H) equations used to assess the shock parameters are vector equations using the vector velocity on both sides of the shock [*Boyd and Sanderson*, 1969]. That information is not available in the ACE real-time data stream. In this paper we describe an alternate analysis that assumes all wind velocities are radial. This permits us to complete the R-H analysis with surprisingly good results. While this adaptation may seem obvious at first, given that the solar wind velocity is primarily in the radial direction, we caution the reader to consider a shock propagating across the solar wind flow direction. In such an instance as the plasma flow changes across the shock there is a natural deflection of the solar wind away from the radial direction in the downstream flow. For high Mach number shocks, this deflection can be significant. It is therefore not obvious that neglecting this deflection will yield acceptable solutions to the R-H equations.

[4] It is vitally important to the development and deployment of a one-component automated analysis that the resulting solutions possess a significant degree of accuracy and reliability over a wide range of parameters in spite of this limitation. Specifically, if all computed shock normals were artificially constrained to lie in the radial direction as a result of not knowing the velocity deflection downstream of the shock, then it is likely that the comparison with the full three-component solutions will be poor and the predicted shock characteristics wrong. The code used here must be capable of computing a best-fit shock normal that lies off the radial direction in spite of the assumption that all measured velocities are radially aligned in order for the analysis to yield acceptable solutions as shocks with normals at large angles to the flow provide the greatest deflection of the wind. We show that for most strong shocks which are expected to be the most geoeffective, this approximation of radial velocity is tolerable. We also find exceptions where significant error is introduced into the analysis.

2. Analysis Method

[5] We employ a multistep analysis method as described by *Vorotnikov et al.* [2008]: identification of shock jump candidates through sustained, abrupt changes in the MHD variables, application of the R-H equations with uncertainties, and evaluation of the quality to which the shock solutions meet the observations. From the solutions we can obtain the shock normal n, shock velocity in the plasma frame $\mathbf{V_P}$, shock velocity in the spacecraft frame $\mathbf{V_S} = \mathbf{V} + \mathbf{V_P}$, Alfvén Mach number $M_A = V_P/V_A$ where V_A is the Alfvén speed, mass flux through the shock surface ρV_P, as well as the density and magnetic field compression ratios $R_n = \rho_{down}/\rho_{up}$ and $R_b = |B|_{down}/|B|_{up}$ where the subscripts "down" and "up" refer to measurements downstream and upstream of the shock, respectively. Shock speed and direction of propagation serve as predictors of shock arrival time at the Earth's magnetopause. Mach number and compression ratios predict how strong the shock will be at arrival. In that paper we compared automated solutions with interactive solutions obtained with the aid of human intervention and decision making assisting in shock recognition and data selection. We found generally good agreement with differences between the automated and interactive solutions at the 1σ level. There were exceptions.

[6] We use a solution method that was originally developed by *Viñas and Scudder* [1986] and then further improved by *Szabo* [1994] wherein we obtain solutions without the need for temperature data. An important final step in the shock analysis is the optimization of the shock solution using all parameters of the upstream and downstream flow. It is this step that is capable of yielding nonradial shock normals in spite of the input assumption that all wind velocities both upstream and downstream of the shock are radial.

[7] The three foremost problems in applying the R-H jump conditions to an automated analysis of spacecraft data are (1) recognizing credible shock candidates, (2) selecting upstream and downstream data points that best characterize the shock jump conditions, and (3) discarding those candidates that prove not to be shocks. We perform the first task by searching for persistent jumps in density, velocity, and temperature and we perform the second task by selecting data points in closest agreement. The third task simply requires solutions to the R-H equations with relatively small uncertainties. The R-H jump expressions are conservation equations and they are valid at every point in the plasma. However, when applied to data not containing a shock jump, the computed density and interplanetary magnetic field (IMF) jumps are small compared with computed uncertainties, the computed Mach number is both subsonic and subAlfvénic, and the shock normal is undetermined (the uncertainty is large). There is little value to a space weather product that "cries

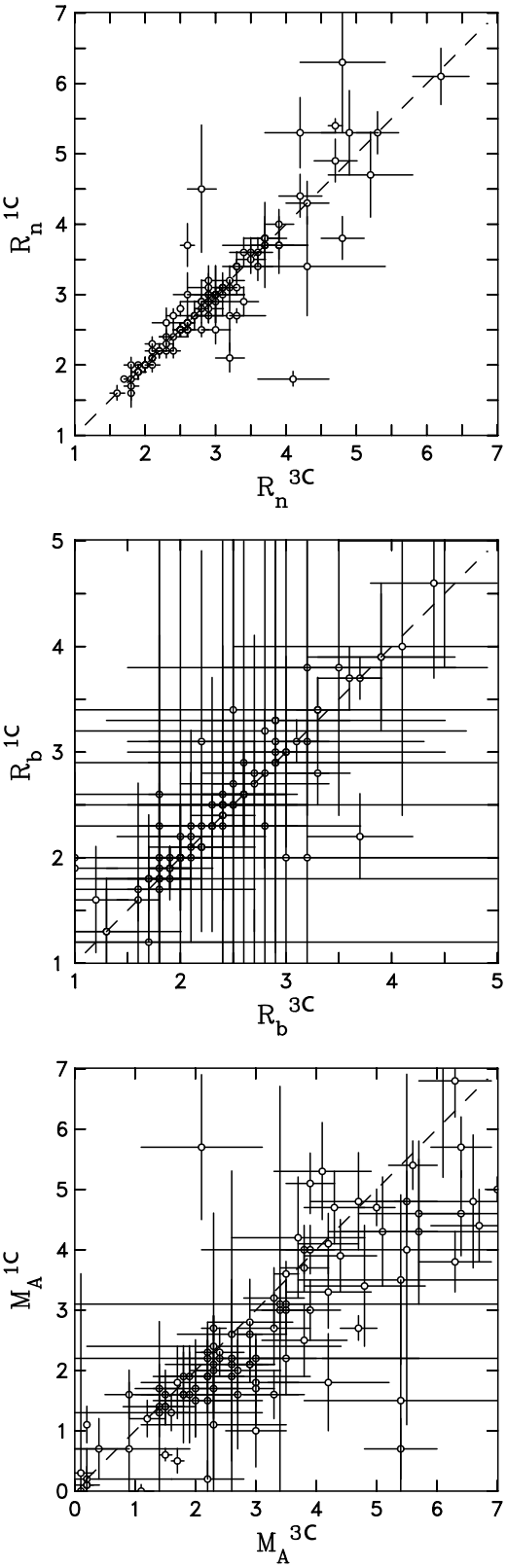

wolf" too often, so in our application software we try to filter out those events that are not well described by our computed R-H solution. Since false shock candidates and weak shocks can yield comparably poor solutions, we insist on solutions with sufficiently small uncertainties so that only the stronger shocks are passed and released to the public. Setting that distinction at a practical level remains an ongoing effort. Strong shocks tend to yield solutions with small relative uncertainties and these are the shocks with the greatest potential for space weather consequences. The analyses shown here focus on shocks with small relative errors in the density and shock speed jumps.

3. Comparison of Solutions

[8] In preparation for a space weather application of the above analysis using ACE real-time data, we make the assumption that the wind velocity both upstream and downstream of the shock is in the radial direction. In other words, we assume that nonradial components of the solar wind velocity are zero. This necessitates straightforward, but physically significant changes to the R-H equations.

[9] The assumption that all wind velocities are radial may appear quite reasonable at first [*Chao and Chen*, 1985; *Volkmer and Neubauer*, 1985]. After all, all wind velocities are essentially radial with only minor deflection at shocks or around obstacles such as CMEs or magnetospheres. However, there can be and generally is a small deflection as described above that is integral to the R-H solution. This analysis is designed to assess the consequences of ignoring that deflection.

[10] We select 95 shocks from the ACE catalog starting from mid-1998 until late 2005. All scored 40 or above in our "goodness of solution test" [*Vorotnikov et al.*, 2008] when using all three components of the solar wind velocity. We analyze them using both the full three-component vector wind velocity technique of *Vorotnikov et al.* [2008] and the new one-component method that assumes all wind velocities are radial and only the speed changes across the shock. Other than this one assumption, all other aspects of the analyses are the same. We use ACE Level-2 data for this analysis in order to obtain the three-component wind velocities needed for comparison.

[11] Figure 1 shows a comparison of the three-component (hereafter referred to as "3C") and one-component (hereafter "1C") automated solutions for the three shock parameters most useful in predicting space weather impact: the

Figure 1. Three shock parameters most useful in space weather calculations: (top) density compression ratio, (middle) magnetic compression ratio, and (bottom) Mach number. Each plot compares the computed parameter for the 1C versus the 3C velocity analysis. Dashed lines here and in Figures 2, 3, 5, and 7 represent equality. The 1C analysis consistently underestimates M_A relative to the 3C analysis.

density compression R_n, the magnetic field compression R_b, and the Mach number M_A. The density compression ratio R_n (Figure 1, top) shows good agreement between the computed values of R_n using the two techniques. However, the uncertainties are generally small for R_n and there are 22 instances where the computed values differ by >1σ and 12 instances where they differ by >2σ. A better measure of the value of a space weather prediction for any given shock might require that R_n be consistent to better than 0.5 and only 10 out of 95 shocks fail this test. Physics requires that these shocks have $1 \le R_n \le 4$. Note that 14 of the shocks yield either 1C or 3C solutions that have $R_n > 4$ while 8 have $R_n > 4$ to better than 1σ. Nine of the 14 shocks have $R_n > 4$ in both solutions. Such unphysical solutions are possible with R-H solvers that do not artificially impose limits on the solutions or allow an operator to seek other solutions. We must attribute such solutions to poor point selection by the automated routine as the interactive solutions whereby data points are hand selected (13 of the 14 shocks have interactive solutions currently) have $R_n < 4$. In spite of the unphysicality of such solutions the two techniques are generally very consistent even in so far as they yield unphysically high values of R_n.

[12] The magnetic compression ratio R_b shown in Figure 1 (middle) is more difficult to assess owing to the larger computed uncertainties. We should note that uncertainties are computed in the normal statistical manner, but the fact that the computed values show less spread than the uncertainties suggests that this technique is flawed in this application. Large computed uncertainties in R_b are a problem with this method regardless of whether one or all three components of the wind velocity are used. They also tend to be larger than uncertainties in R_n in interactive solutions done with greater care and human intervention. Three of the 95 shocks have computed values of R_b that differ by >1σ and only 1 has values that differ by >2σ. Neglecting the large uncertainties, only eight computed values of R_b derived from the two methods disagree by more than 50% and 66 agree to better than 10%. The computed values of R_b differ by more than 0.5 in 20 out of 95 shocks. Proper shock solutions are also limited to $R_b < 4$ and some of these solutions suffer from the violation of this constraint as well for the same reason that we find $R_n > 4$.

[13] The Alfvén Mach number M_A shown in Figure 1 (bottom) shows generally good agreement between the two sets of solutions, but there is a systematic shift showing a tendency for $M_A^{3C} > M_A^{1C}$. The interpretation of a few shocks is complicated by large uncertainties and there are several events that show strong disagreement between

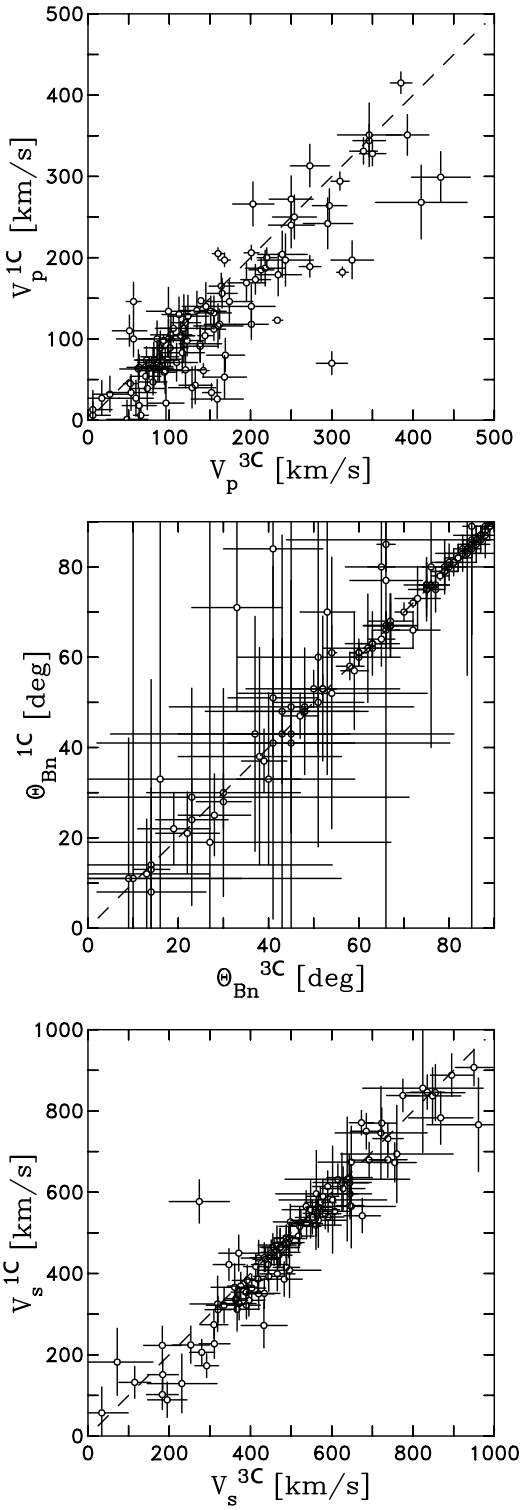

Figure 2. Three shock parameters necessary in computing shock arrival time at Earth assuming planar shock: (top) shock speed in plasma frame, (middle) angle between shock normal and mean magnetic field (as a proxy comparison to shock normal vector), and (bottom) shock speed in spacecraft frame. Each plot compares the computed parameter for the 1C versus the 3C velocity analysis. The 1C analysis consistently underestimates shock speeds V_p and V_s relative to the 3C analysis.

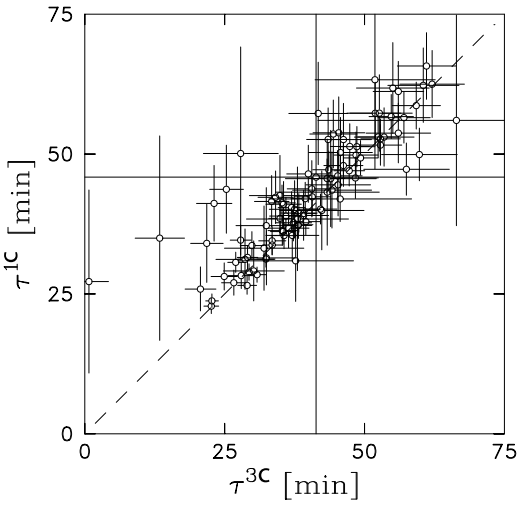

Figure 3. Comparison of arrival time predictions using 3C and 1C wind analyses. Note that 1C analyses consistently overestimate arrival times relative to the 3C analysis owing to the corresponding underestimation of shock speed.

the two solutions. Thirty-two shocks show disagreement in the computed values of M_A at >1σ level while 16 show disagreement at >2σ. Neglecting errors, 26 (78) shocks have differences in computed values of M_A that are less than 10% (50%) of their mean. The physical constraint on M_A is $M_A \geq 1$ and a strong interplanetary shock can reach $M_A = 5$ or higher, so we ask how many solutions disagree by a value more than 1 and that answer is 29.

[14] Figure 2 shows the comparison of the three shock parameters needed to compute shock arrival times. The shock speed in the plasma frame V_p shows remarkably good agreement between the two analyses, although as with M_A there is a general shift toward $V_p^{3C} > V_p^{1C}$. Uncertainties are small and 43 of the 95 pairs of shock solutions show a difference between the two computed values of V_p at >1σ level. Twenty solutions disagree at >2σ level while only 16 of the 20 show differences in V_p greater than 50 km/s (the nominal Alfvén speed at 1 AU).

[15] The computed shock normals are compared in the form of Θ_{Bn}, the angle between the shock normal and the upstream mean magnetic field, shown in Figure 2 (middle). Uncertainties are an unusual admixture of the very large and the very small with the quasi-perpendicular solutions showing the consistently smaller uncertainties. Only three of the 95 Θ_{Bn} pairs disagree by >1σ and only one disagrees by >2σ, but the computed uncertainties are large. Perhaps more significantly, only five shocks have values of Θ_{Bn} that differ by more than 10° and only one differs by more than 20°. This suggests that the assumption limiting the solar wind velocity to the radial component is not significantly altering the computed shock normal in most cases.

[16] The computed shock speed in the spacecraft frame V_s shown in Figure 2 (bottom) shows good agreement between the two solution methods with generally small uncertainties. Again, there is a tendency for $V_s^{3C} > V_s^{1C}$, but the systematic shift is small. While 24 pairs of V_s show disagreements at >1σ level, only 4 show disagreement at >2σ level. This suggests that the predicted arrival times at the Earth's magnetopause should be in good agreement between the two sets of solution.

[17] We can then ask to what degree the differences between the solutions may alter the predicted arrival time of the shock at the Earth's magnetopause. Assuming a planar shock and ignoring magnetopause curvature, we compute the transit time from L_1 to the magnetopause subsolar point and compare results for the 3C and 1C solutions. The transit time τ is given as

$$\tau = Dn_R/V_s, \tag{1}$$

where

$$V_s = V_p + V_{SW}n_R, \tag{2}$$

D is the distance from the magnetosphere's subsolar point to L_1 and n_R is radial component of the shock normal (assumed positive).

[18] A comparison of transit times computed using the 3C and 1C analyses is shown in Figure 3. Twenty-four shocks disagree by >1σ, while only three shocks show disagreement at >2σ level. Twenty-eight shock arrival times differ by more than 10 min, 4 differ by more than 20 min, and only 1 out of 95 differs by more than 30 min. There is a slight bias toward later arrival times in the 1C model, which can be attributed to the tendency for $V_s^{3C} > V_s^{1C}$, although in the majority of instances the difference is not statistically significant. However, this should be considered carefully due to the importance of accurate arrival time predictions in the functioning of a space weather warning system and the possibility of a shock arriving earlier than computed using the 1C model.

[19] It is a simple matter to diagnose the disagreement in transit times derived for the two analyses as there are only two variables involved: n_R and V_s. We have compared the shock normals for the two analyses. In only 4 out of 95 shocks is $\mathbf{n}^{3C} \cdot \mathbf{n}^{1C} < 0.98$ ($\Theta_{n^{3C}n^{1C}} > 11.5°$). In only 5 out of 95 shocks is $\mathbf{n}^{3C} \cdot \mathbf{n}^{1C} < 0.99$ ($\Theta_{n^{3C}n^{1C}} > 8.1°$). There is no strong, systematic correlation between this difference and the orientation of the shock normal relative to the solar wind. The difference in shock normals is not the root cause of the transit time differences in most cases. In most instances, the differences in computed transit times derive from slow plasma frame speeds computed in the 1C analysis, but we find no consistent reason for these slow shock speed solutions.

[20] There are approximately eight solutions in Figure 3 with large errors and predicted transit times that are much longer in the 1C analyses. One shock stands out (0652 UT on day 1998/275) with transit times 0.7 and 27.2 min in the 3C and 1C analyses, respectively. While it is especially noteworthy that the almost immediate arrival prediction is

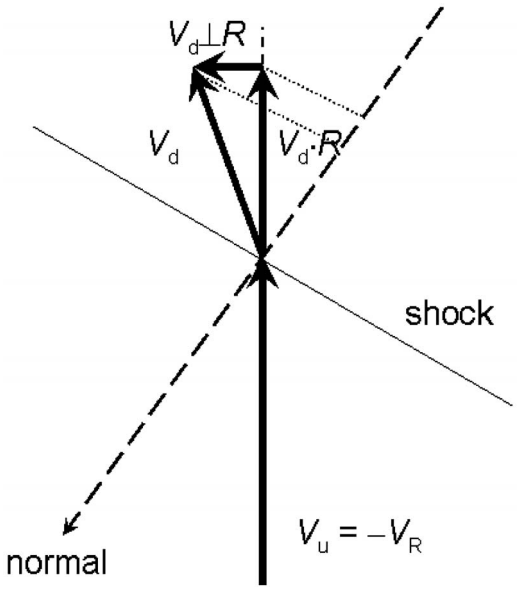

Figure 4. Demonstration of how limitation of the flow to the *R* component results in an overestimation of the downstream normal component and the resulting shock speed.

derived from the 3C analysis, the source of the difference is shown in the next plot where the angles between the computed shock normal and the radial direction are 89.6° and 81.9°, respectively. The interactive shock solution determines Θ_{Rn} = 73° suggesting the unexpected result that the 1C automated analysis is superior to the 3C solution.

[21] There can be only one source for the discrepancies seen between the 3C and 1C analyses and that is the omission of the *T* and *N* components of the flow vector. In general, the upstream flow parallel to the shock normal is correctly given by the projection of the *R* component of the wind onto the normal direction. This is the same in the 3C and 1C analyses. If we neglect the magnetic field and perform a simple analysis in the spacecraft frame, the downstream flow in the hydrodynamic solution is deflected away from the shock normal and into the (*T*, *N*) plane where it is unreported in the real-time data stream. Figure 4 shows what happens. The normal component of the flow decreases in the downstream region while the component coplanar to the shock surface is preserved. This results in a deflection of the flow away from the normal vector. Decomposing the downstream flow vector into the unnatural basis set (*R*, *T*, *N*) reveals that the *R* component alone overestimates the normal component while the *T* and *N* components tend to reduce the computed normal component. The resulting estimate for the downstream flow parallel to the shock normal is *overestimated* by the 1C analysis. Since V_s is the difference between upstream and downstream normal component flow, we get the observed result that $V_s^{3C} > V_s^{1C}$. There are two notable exceptions. In the case of Θ_{Rn} = 0° and propagation of the shock along the radial direction, there is no downstream flow deflection away from the radial direction. Therefore, the downstream flow is correctly measured by the 1C analysis. In the case of Θ_{Rn} = 90° and propagation across the *R* direction, there can be no additional deflection away from the normal as the downstream flow is limited to be within 90° of the normal. However, in this instance the upstream flow is no longer correctly determined either as the *R* component is now perpendicular to the shock normal. In this instance the flow on both sides of the shock is unsampled and the 1C solution is poorly constrained. The latter instance represents only a small fraction of configuration space as shocks with normals perpendicular to the *R* direction are very few. Restoration of the magnetic field will modify the downstream flow deflection, but it is not expected to be a large effect for low Mach number interplanetary shocks.

[22] In the end, the failure of the two methods to agree can be traced to three classes of disagreement between the analyses. First, there is a systematic shift with slower shock speeds computed in the 1C analysis as detailed above. Second, there is an error in the 1C analysis for shock normals highly orthogonal to the radial direction ($\Theta_{Rn} \simeq 90°$) that is most likely attributable to the final stage of the shock analysis that seeks to optimize the shock solution subject to undersampled conservation relations as discussed above. Third, there also exists an occasional error at arbitrary angles of propagation that we find difficult to diagnose or predict. With these explanation in mind, we present the following diagnostics.

[23] Figure 5 shows a comparison of Θ_{Rn} computed from the 3C and 1C methods. The two analyses yield close agreement on the shock normals in most cases with small disagreements when the shock normal forms a large angle

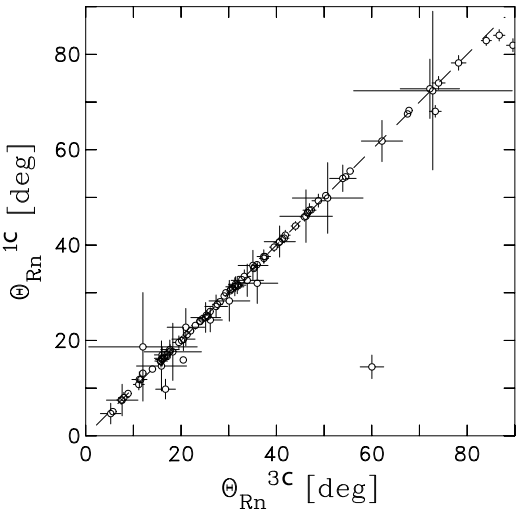

Figure 5. Comparison of computed angle between shock normal and radial direction using the 3C and 1C wind analyses.

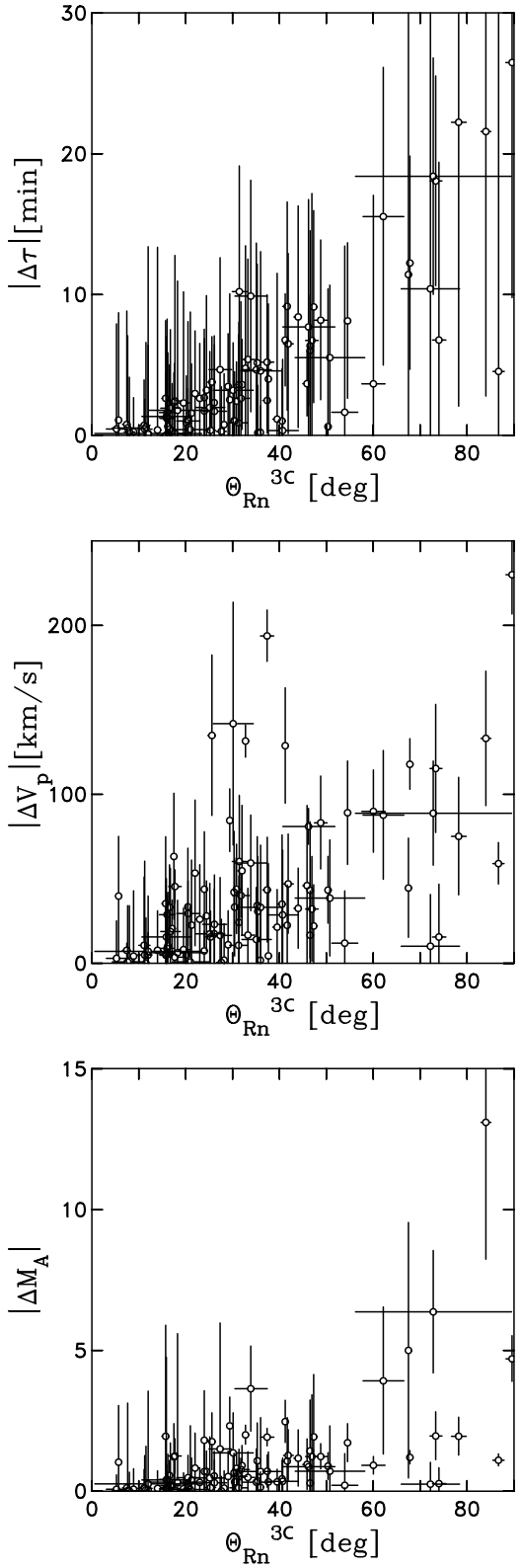

Figure 6. Difference between 3C and 1C analyses for shock parameters relevant to arrival time calculation. (top) Difference in predicted arrival time $|\Delta\tau|$ as a function of Θ_{Rn} computed using the 3C method. (middle) Difference in computed plasma frame shock speed $|\Delta V_p|$ as a function of Θ_{Rn} computed using the 3C method. (bottom) Difference in computed shock Mach number $|\Delta M_A|$ as a function of Θ_{Rn} computed using the 3C method.

to the radial direction Θ_{Rn}. The day 2000/224 shock is clearly seen in the lower right part of the panel as having the greatest departure from the line. All other shocks seem to be in relatively good agreement. Therefore, it would seem there is no strong systematic inability to determine the shock normal and only occasional disagreement between the two analyses.

[24] Figure 6 plots the difference in the computed arrival times $|\Delta\tau|$, shock speeds in the plasma frame $|\Delta V_p|$, and Alfvén Mach number $|\Delta M_A|$ as a function of Θ_{Rn} computed from the 3C analysis. Note that in all three instances the discrepancy is small when $\Theta_{Rn} \simeq 0°$ as expected from the above argument. What is seen is a systematic error associated with increasing Θ_{Rn}. The high Θ_{Rn} values that show large discrepancies between the arrival times computed for the 3C and 1C analyses are the same points that appear well above the line in Figure 3. It is not an error in the shock normal, but in the shock speed that is the problem. When $\Theta_{Rn} \simeq 90°$ arrival time is dominated by shock propagation speed in the plasma frame V_p and not convection. This is precisely the term that is poorly resolved by the 1C analysis. The plot of V_p versus Θ_{Rn} clearly shows a systematic error at large values of Θ_{Rn}. How large Θ_{Rn} must be for propagation to dominate convection depends on the wind speed, but what are more important are the errors that develop in the shock solutions at large angles of propagation. This error is best illustrated by the $|\Delta M_A|$ result.

[25] The plot of $|\Delta V_p|$ versus Θ_{Rn} also shows five events with high and seemingly random errors in the range $20° < \Theta_{Rn} < 40°$. Examination of these solutions reveals relatively good agreement between the computed values of τ, R_n, and R_b, but does show disagreement in the computed V_p, V_s, and M_A. We can find no systematic source for these disagreements. Fortunately, the variability in actual transit time to Earth is limited, and for the purpose of space weather alerts an accurate assessment of shock compression is more important than shock speed.

[26] Finally, we can compare our predicted arrival times to measured shock arrival times as determined from ground-based magnetometers [*Yumoto and the CPMN Group*, 2001; *Solovyev et al.*, 2004] using the 210 mm and IMAGE chains. We look for sudden commencements in the horizontal component of ground level measurements in association with each shock observation and assume a ±3 min uncertainty in the result due to background fluctuations and ambiguities in initial risetime. Figure 7 shows

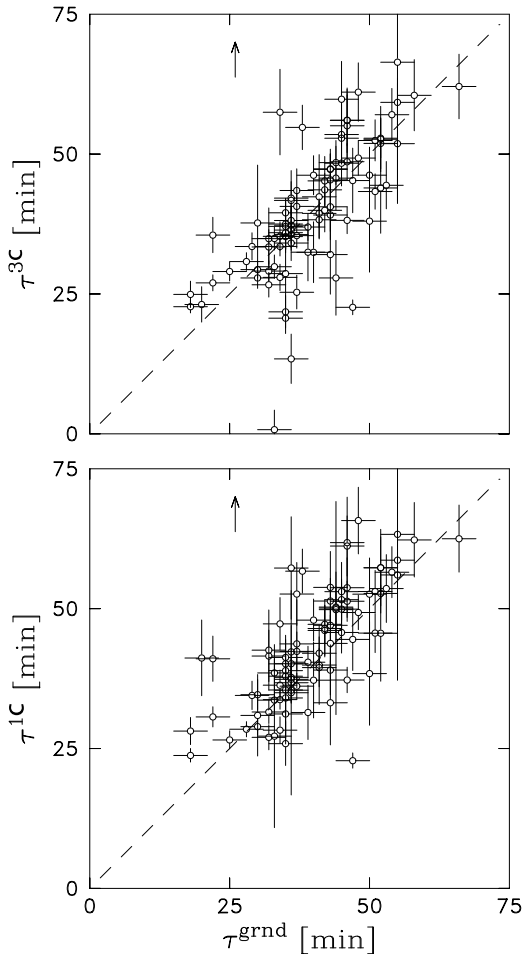

Figure 7. Predicted arrival times in (top) 3C analysis and (bottom) 1C analysis as compared with measured arrival times using ground-based magnetometers. While there are a few notably poor predictions, most solutions in both the 3C and 1C analyses yield reasonable arrival times in good agreement with observations.

that comparison. One shock is omitted from both the 3C and 1C panels as the predicted transit times (~198 and ~78 min, respectively) are significantly off scale. These solutions are consistently poor for reasons unknown and are represented by arrows in the panels. To leading order most 1C and 3C predictions compare favorably with the observations with shock arrival times dominated by convection. Predictions derived from the 1C analysis tend to be slightly longer than the 3C predictions which reflects the conclusions drawn from Figures 3–6 where it is seen that shock speeds are consistently slower in the 1C than in the 3C analysis. This systematic shift of ~5 minutes or less does not negate the value of the 1C analysis in space weather applications, but should be kept in mind. Both analyses are more than capable of yielding poor arrival time predictions and we believe this reflects data point selection at the leading step in the analysis rather than systematic flaws in the analysis. At present we know of no way to improve this aspect of the analysis, but we are working on it.

4. Summary

[27] The purpose of this paper has been to show that good solutions to the R-H equations can be obtained using only the wind speed in place of the three-component wind velocity by assuming that all wind velocities are radial. However, we have seen that there are exceptions to this rule that can have significant space weather consequences. Shocks having large angles between their normal vectors to the radial direction can result in significant error between the fully three-component R-H analysis and the reduced one-component wind speed analysis. This tends to lead to differences in computed shock speed while it only occasionally leads to significant differences in predicted arrival times. We note there are a few seemingly random occurrences of disagreement (error) that fit no particular pattern. We attribute these errors to data point selection, but the complete answer is probably more complicated. The inability to predict when some shock solutions may diverge is troubling and we continue to study the problem. Our current data selection method looks for subsets of the measurements before and after the shock that show the greatest consistency. This is an attempt to remove fluctuations from the low time resolution data. This selection method does not always yield an acceptable solution, although *Vorotnikov et al.* [2008] do show that it works in general. This is a viable technique for space weather applications, but more is needed to improve the reliability of the technique. Perhaps most importantly, we caution all readers to be aware that shocks of textbook quality are rare and complications such as changing plasma conditions are common. One should view all shock solutions with a healthy skepticism and automated solutions particularly so. While they are useful, their accuracy should always be suspect.

[28] While this effort remains a work in progress and we hope to improve the overall performance of the automated analysis routines, we have developed a web page and supporting automated scripts to run shock analyses in real time and provide the solutions to the public for space weather applications. That web page, which operates as part of the ACE Science Center is http://www.srl.caltech.edu/ACE/ASC/DATA/Shocks/shocks.html. Solar minimum provides very few strong shocks, but several recent weak shocks have been observed and we must report that they failed our detection analysis. This failure is in part by design to avoid false positive reports, but we now understand that transients with poor shock solutions such as simple pressure pulses may still have significant space weather consequences and we are working to broaden the scope of our real-time reporting. As solar maximum comes on we hope to gain added experience and refine our selection and reporting criteria. In the meantime, we

will continue to provide these solutions to the public for use in space weather applications.

[29] **Acknowledgments.** Funding for this work was provided by NASA grants NNG04GMO5G and NAG5-12492 and Caltech subcontract 44A-1062037 in support of the ACE/MAG experiment. Support at LANL was provided under the auspices of the U.S. Department of Energy, with financial support from the NASA ACE program. We thank the Solar-Terrestrial Laboratory at Nagoya University for providing the 210MM magnetic observations and the IMAGE ground-based magnetometer team for providing data used in this study. V.S.V. was an undergraduate senior at UNH pursuing a chemical engineering major in renewable energy when this work was performed. He is now a graduate student in the Center for Renewable Energy at the University of Delaware. C.J.M. was a visiting undergraduate at UNH at the time this work was completed.

References

Balch, C. C. (2008), Updated verification of the Space Weather Prediction Center's solar energetic particle prediction model, *Space Weather*, *6*, S01001, doi:10.1029/2007SW000337.

Boyd, T. J., and J. J. Sanderson (1969), *Plasma Dynamics*, Barnes and Noble, New York.

Chao, J. K., and Y. H. Chen (1985), On the distribution of Θ_{Bn} for shocks in the solar wind, *J. Geophys. Res.*, *90*, 149–153.

Huttunen, K. E. J., S. P. Kilpua, A. Pulkkinen, A. Viljanen, and E. Tanskanen (2008), Solar wind drivers of large geomagnetically induced currents during the solar cycle 23, *Space Weather*, *6*, S10002, doi:10.1029/2007SW000374.

Smith, Z. K., T. R. Detman, W. Sun, M. Dryer, C. S. Deehr, and C. D. Fry (2008), Modeling the arrival at Earth of the interplanetary shock following the 12 May 1997 solar event using HAFv2 and 3-D MHD HHMS models, *Space Weather*, *6*, S05006, doi:10.1029/2007SW000356.

Solovyev, S. I., A. V. Moiseyev, V. A. Mullayarov, A. Du, M. Engebretson, and L. Newitt (2004), Global geomagnetic response to a sharp compression of the magnetosphere and IMF variations on October 29, 2003, *Cosmic Res.*, *42*, 597–606.

Sun, W., C. S. Deehr, M. Dryer, C. D. Fry, Z. K. Smith, and S.-I. Akasofu (2008), Simulated Solar Mass Ejection Imager and "Solar Terrestrial Relations Observatory-like" views of the solar wind following the solar flares of 27–29 May 2003, *Space Weather*, *6*, S03006, doi:10.1029/2006SW000298.

Szabo, A. (1994), An improved solution to the "Rankine-Hugoniot" problem, *J. Geophys. Res.*, *99*, 14,737–14,746.

Viñas, A. F., and J. D. Scudder (1986), Fast and optimal solution to the "Rankine-Hugoniot problem", *J. Geophys. Res.*, *91*, 39–58.

Volkmer, P. M., and F. M. Neubauer (1985), Statistical properties of fast magnetoacoustic shock waves in the solar wind between 0.3 AU and 1 AU—HELIOS-1,2 observations, *Ann. Geophys.*, *3*, 1–12.

Vorotnikov, V. S., C. W. Smith, Q. Hu, A. Szabo, R. M. Skoug, and C. M. S. Cohen (2008), Automated shock detection and analysis algorithm for space weather application, *Space Weather*, *6*, S03002, doi:10.1029/2007SW000358.

Yu, Y., and A. J. Ridley (2008), Validation of the space weather modeling framework using ground-based magnetometers, *Space Weather*, *6*, S05002, doi:10.1029/2007SW000345.

Yumoto, K., and the CPMN Group (2001), Characteristics of Pi 2 magnetic pulsations observed at the CPMN stations: A review of the STEP results, *Earth Planets Space*, *53*, 981–992.

Zwickl, R. D., et al. (1998), The NOAA Real-Time Solar-Wind (RTSW) system using ACE data, *Space Sci. Rev.*, *86*(1–4), 633–648.

C. M. S. Cohen and A. J. Davis, Space Radiation Laboratory, California Institute of Technology, MC 220-47, 1200 E. California Ave., Pasadena, CA 91125, USA. (cohen@srl.caltech.edu; ad@srl.caltech.edu)

C. J. Farrugia and C. W. Smith, Space Science Center, Institute for the Study of Earth, Oceans, and Space, Physics Department, Morse Hall, University of New Hampshire, Durham, NH 03824, USA. (charlie.farrugia@unh.edu; charles.smith@unh.edu)

Q. Hu, CSPAR, University of Alabama in Huntsville, 320 Sparkman Dr., Huntsville, AL 35805, USA. (qh0001@uah.edu)

C. J. Meredith, Department of Physics and Astronomy, University of Leicester, Leicester LE17RH, UK. (cjm49@leicester.ac.uk)

R. M. Skoug, Los Alamos National Laboratory, MS D466, Los Alamos, NM 87545, USA. (rskoug@lanl.gov)

A. Szabo, Code 672, NASA Goddard Space Flight Center, Greenbelt, MD 20771, USA. (adam.szabo@nasa.gov)

V. S. Vorotnikov, Department of Chemical Engineering, University of New Hampshire, Durham, NH 03824, USA. (vasya@udel.edu)

K. Yumoto, Space Environment Research Center, Kyushu University, 6-10-1 Hakozaki, Fukuoka 812-8581, Japan. (yumoto@serc.kyushu-u.ac.jp)